Supporting information

Assessment of ATP8B1 deficiency in pediatric patients with cholestasis using macrophages

Hisamitsu Hayashi,[1,*] Sotaro Naoi,[1,*] Takao Togawa,[2] Yu Hirose,[1] Hiroki Kondou,[3] Yasuhiro Hasegawa,[4] Daiki Abukawa,[5] Mika Sasaki,[6] Koji Muroya,[7] Satoshi Watanabe,[8] Satoshi Nakano,[9] Kei Minowa,[9] Ayano Inui,[10] Akinari Fukuda,[11] Mureo Kasahara,[11] Hironori Nagasaka,[12] Kazuhiko Bessho,[4] Mitsuyoshi Suzuki,[9] and Hiroyuki Kusuhara[1]

(H.H. and S.N. contributed equally to this work.)

[1]Laboratory of Molecular Pharmacokinetics, Graduate School of Pharmaceutical Sciences, The University of Tokyo, Tokyo, Japan; [2]Department of Pediatrics and Neonatology, Nagoya City University Graduate School of Medical Sciences, Nagoya, Japan; [3]Department of Pediatrics, Nara Hospital, Kinki University Faculty of Medicine, Nara, Japan; [4]Department of Pediatrics, Osaka University Graduate School of Medicine, Osaka, Japan; [5]Department of General Pediatrics, Miyagi Children's Hospital, Miyagi, Japan; [6]Department of Pediatrics, School of Medicine, Iwate Medical University, Iwate, Japan; [7]Department of Endocrinology and Metabolism, Kanagawa Children's Medical Center, Kanagawa, Japan; [8]Department of Pediatrics, Nagasaki University Hospital, Nagasaki, Japan; [8]Department of Pediatrics, Nagasaki University Hospital, Nagasaki, Japan; [9]Department of Pediatrics, Juntendo University School of Medicine, Tokyo, Japan; [10]Department of Pediatric Hepatology and Gastroenterology, Eastern Yokohama Hospital, Kanagawa, Japan; [11]Organ Transplantation Center, National Center for Child Health and Development, Tokyo, Japan; [12]Department of Pediatrics, Takarazuka City Hospital, Hyogo, Japan.

Keywords; pediatric liver disease; diagnosis; progressive familial intrahepatic cholestasis

Contact information: Hisamitsu Hayashi, Ph.D., Assistant Professor, Laboratory of Molecular Pharmacokinetics, Department of Medical Pharmaceutics, Graduate School of Pharmaceutical Sciences, The University of Tokyo, 7-3-1 Hongo, Bunkyo-ku, Tokyo 113-0033, Japan, Phone: +81-3-5841-4771, Fax: +81-3-5841-4766, E-mail: hayapi@mol.f.u-tokyo.ac.jp

List of abbreviations: BSEP, bile salt export pump; GGT, gamma-glutamyl transferase; HA, hemagglutinin; HBV, hepatitis B virus; HCV, hepatitis C virus; HMDM, human peripheral blood monocyte-derived macrophages; HPBMo, human peripheral blood monocytes; LTx, liver transplantation; PFIC, progressive familial intrahepatic cholestasis; PM, plasma membrane; qPCR, quantitative PCR; siRNA, short interfering RNA; STAT3, signal transducer and activator of transcription 3

Materials and methods

Plasmids

The pShuttle vector containing human ATP8B1 cDNA C-terminally tagged with FLAG (pShuttle–ATP8B1^{WT}-FLAG) and human CDC50A N-terminally tagged with a hemagglutinin antigen (HA) (pShuttle–HA–CDC50A) were constructed as described previously.(Hasegawa et al., 2014) Site-directed mutagenesis was performed as described previously(Hayashi et al., 2012a, Hayashi and Sugiyama, 2009, Hayashi et al., 2005) to introduce the c.916T>C (p.C306R), c.2941G>A (p.E981K), or c.234C>G (p.H78Q), c.1729A>G (p.I577V), and c.2021T>C (p.M674T), mutations into ATP8B1^{WT}–FLAG (ATP8B1^{C306R}–FLAG, ATP8B1^{E981K}–FLAG, or ATP8B1^{Triple}–FLAG).

Sequence analysis of *ATP8B1*, *ABCB11, and* the genes responsible for neonatal/infantile intrahepatic cholestasis.

Genomic DNA was isolated from peripheral blood leukocytes using a Wizard Genomic DNA Purification Kit (Promega, Madison, WI), and all exons and flanking intron–exon boundaries of the genes responsible for neonatal/infantile intrahepatic cholestasis including *ATP8B1* and *ABCB11* were analyzed by targeted next-generation sequencing(Togawa et al., 2016) and/or Sanger sequencing,(Hasegawa et al., 2014, Naoi et al., 2014) as described previously.

Preparation of cell lysates from HMDM after IL-10 stimulation

60 min after IL-10 stimulation, the HMDM were lysed with cell lysis buffer (Cell Signaling technology, Danvers, MA) supplemented with protease inhibitor cocktails (Sigma-Aldrich, St. Louis, MO) and phosphatase inhibitor cocktail (Cell Signaling technology).

Preparation of membrane fractions from liver specimens

Liver specimens from the patients were homogenized in hypotonic buffer (1 mM EDTA, 5 mM sodium phosphate, pH 7.0) supplemented with protease inhibitor cocktails (Sigma-Aldrich) using a QIAshredder (Qiagen, Valencia, CA), and then centrifuged at 800×g for 10 min at 4°C. The supernatant was ultracentrifuged at 100,000×g for 1 h at 4°C and the pellets were lysed and subjected to the immunoblotting.

Cell surface biotinylation

Cell surface biotinylation to prepare cell surface fractions was performed as previously reported.(Hayashi et al., 2012a, Hayashi et al., 2012b) Isolated biotinylated protein was analyzed by immunoblotting.

Immunoblotting

Specimens were loaded into wells of an 8% SDS-polyacrylamide gel (SDS-PAGE) with a 3.75% stacking gel, electrophoresed, and subjected to immunoblotting as described previously.(Hayashi et al., 2012b, Matsuzaka et al., 2015) The intensity of the band indicating each protein was quantified using MultiGauge software (v. 2.0; Fujifilm, Tokyo, Japan).

Flow cytometry

Nonpolarized or IL-10-treated HMDM adhered to Repcell dishes were harvested by incubating the dishes on ice. The collected cells were suspended in FACS buffer (PBS (–) containing 5 % human AB serum, 1 mM EDTA-2Na, and 0.1 % sodium azide), incubated on ice for 15 min with BD human Fcblock (BD Biosciences, San Jose, CA), and stained on ice for 90 min with fluorochrome-labelled antibodies. For analysis of the intracellular expression

of CD68, cells stained with antibodies against cell surface molecules were fixed and permeabilized using BD Cytofix/Cytoperm™ Fixation/Permeabilization Solution, washed with BD Perm/Wash™ Buffer, and stained with anti-CD68-FITC. Isotype control labeling was performed in parallel. Data for the stained cells were acquired on a BD FACSAria II Cell Sorter (BD Biosciences) and analyzed using FlowJo software (v. 10; Tree Star, San Carlos, CA). Macrophages were gated based on their forward scatter (FSC) and side scatter (SSC) properties. More than 95% of the gated cells were positive for the macrophage marker CD68 (Supporting Fig. 2). Values are expressed as the ratio of the mean fluorescence intensity (MFI) of the marker of interest to the MFI of the isotype control.

Quantitative PCR (qPCR)

RNA was isolated using RNeasy Mini kits (Qiagen) according to the manufacturer's instructions. Reverse transcription was performed using ReverTra Ace® qPCR RT Master Mix with gDNA Remover (Toyobo, Osaka, Japan). The level of mRNA expression of the target genes was determined by real-time qPCR using a LightCycler 480 system II (Roche Diagnostics, Mannheim, Germany), the appropriate software (v. 3.53; Roche Diagnostics), and Thunderbird SYBR qPCR Mix (Toyobo) as described previously.(Matsuzaka et al., 2015) The primer sequences used are listed in Supporting Table 2. Gene expression for each reaction was normalized to the expression of human *β-actin (ACTB)*.

Immunocytochemistry

HMDM treated with or without IFN-γ and IL-10, and the transfected CHO-K1 cells were cultured on glass coverslips (Matsunami Glass Inc. Ltd, Osaka, Japan) in 12-well plates, stained, and visualized using a Leica TCS SP5 II laser scanning confocal microscope (Leica Microsystems, Solms, Germany) as described previously.(Hasegawa et al., 2014)

Flippase assay

The flippase activity of ATP8B1 was evaluated by incorporation of nitrobenzoxadiazole-labeled phosphatidylcholine (NBD-PC; Avanti Polar Lipids, Alabaster, AL) into the inner leaflet of the plasma membranes (PM) using flow cytometry as described previously(Takatsu et al., 2014). In brief, 48 h after the transfection, CHO-K1 cells were detached from dishes in PBS containing 5 mM EDTA, suspended in 500 μl of Hanks' balanced salt solution (pH 7.4) containing 1 g/l glucose (HBSS-glucose), and equilibrated at 15 °C for 15 min. The suspended cells were added to an equal volume of 2 μM NBD-PC in HBSS-glucose and incubated at 15 °C for the indicated period. At each time point, 400 μl of cell suspension was collected, mixed with 400 μl of ice-cold HBSS-glucose containing 5% fatty acid-free BSA, and incubated on ice for 5 min to extract the NBD-PC from the outer leaflet of the PM and the unincorporated NBD-PC. Then, the cells were stained with propidium iodide (PI) for 40 min on ice. MFI were calculated for 10,000 cells in each specimen. Data were acquired on a BD FACSAria II Cell Sorter and analyzed using FlowJo software (v. 10). PI-positive cells were excluded from the analysis.

References

HASEGAWA, Y., HAYASHI, H., NAOI, S., KONDOU, H., BESSHO, K., IGARASHI, K., HANADA, K., NAKAO, K., KIMURA, T., KONISHI, A., NAGASAKA, H., MIYOSHI, Y., OZONO, K. & KUSUHARA, H. 2014. Intractable itch relieved by 4-phenylbutyrate therapy in patients with progressive familial intrahepatic cholestasis type 1. *Orphanet J Rare Dis,* 9**,** 89.

HAYASHI, H., INAMURA, K., AIDA, K., NAOI, S., HORIKAWA, R., NAGASAKA, H., TAKATANI, T., FUKUSHIMA, T., HATTORI, A., YABUKI, T., HORII, I. & SUGIYAMA, Y. 2012a. AP2 adaptor complex mediates bile salt export pump internalization and modulates its hepatocanalicular expression and transport function.

Hepatology, 55**,** 1889-900.

HAYASHI, H., NAOI, S., NAKAGAWA, T., NISHIKAWA, T., FUKUDA, H., IMAJOH-OHMI, S., KONDO, A., KUBO, K., YABUKI, T., HATTORI, A., HIROUCHI, M. & SUGIYAMA, Y. 2012b. Sorting nexin 27 interacts with multidrug resistance-associated protein 4 (MRP4) and mediates internalization of MRP4. *J Biol Chem,* 287**,** 15054-65.

HAYASHI, H. & SUGIYAMA, Y. 2009. Short-chain ubiquitination is associated with the degradation rate of a cell-surface-resident bile salt export pump (BSEP/ABCB11). *Mol Pharmacol,* 75**,** 143-50.

HAYASHI, H., TAKADA, T., SUZUKI, H., AKITA, H. & SUGIYAMA, Y. 2005. Two common PFIC2 mutations are associated with the impaired membrane trafficking of BSEP/ABCB11. *Hepatology,* 41**,** 916-24.

MATSUZAKA, Y., HAYASHI, H. & KUSUHARA, H. 2015. Impaired Hepatic Uptake by Organic Anion-Transporting Polypeptides Is Associated with Hyperbilirubinemia and Hypercholanemia in Atp11c Mutant Mice. *Mol Pharmacol,* 88**,** 1085-92.

NAOI, S., HAYASHI, H., INOUE, T., TANIKAWA, K., IGARASHI, K., NAGASAKA, H., KAGE, M., TAKIKAWA, H., SUGIYAMA, Y., INUI, A., NAGAI, T. & KUSUHARA, H. 2014. Improved liver function and relieved pruritus after 4-phenylbutyrate therapy in a patient with progressive familial intrahepatic cholestasis type 2. *J Pediatr,* 164**,** 1219-1227 e3.

TAKATSU, H., TANAKA, G., SEGAWA, K., SUZUKI, J., NAGATA, S., NAKAYAMA, K. & SHIN, H. W. 2014. Phospholipid flippase activities and substrate specificities of human type IV P-type ATPases localized to the plasma membrane. *J Biol Chem,* 289**,** 33543-56.

TOGAWA, T., SUGIURA, T., ITO, K., ENDO, T., AOYAMA, K., OHASHI, K., NEGISHI, Y., KUDO, T., ITO, R., KIKUCHI, A., ARAI-ICHINOI, N., KURE, S. & SAITOH, S. 2016. Molecular Genetic Dissection and Neonatal/Infantile Intrahepatic Cholestasis Using Targeted Next-Generation Sequencing. *J Pediatr,* 171**,**

171-177 e4.

Supporting figure legends

Supporting Fig. 1. Differentiation of HPBMo into HMDM.

HPBMo were seeded and differentiated into HMDM by culture for 9 days in RPMI/M-CSF (a, b), and then cultured for 6 days in RPMI/M-CSF with or without IFN-γ (40 ng/ml) (c). (a, b) Differentiation of HPBMo into HMDM. (a) Morphological changes. Photomicrographs were taken 1, 3, 6, and 9 days after seeding HPBMo. Scale bar, 50 μm. (b) Expression of monocyte and macrophage markers. One or 9 days after seeding HPBMo, the cells were fixed and immunostained for confocal microscopy with antibodies against CD93 (monocyte marker) and 25F9 (macrophage marker), as described in the Supporting information. Scale bar, 20 μm. (c) Polarization of HMDM into M1. The cells were fixed and immunostained for confocal microscopy with antibodies against CD80 (M1 marker). Scale bar, 20 μm. In (a–c), a representative result of at least two independent experiments is shown.

Supporting Fig. 2. Correct differentiation of ATP8B1-deficient HPBMo into HMDM.

HMDM transfected with siControl or siATP8B1 (a) and HMDM from control subjects or patients with PFIC1 (b) were generated as described in Fig. 2 and 5, respectively. The cells were cultured in RPMI/M-CSF with or without IL-10 (40 ng/ml) for the last 6 days and then stained with fluorochrome-labeled antibodies against CD68, a pan-macrophage marker, and CD93, a monocyte marker, subjected to flow cytometry, and analyzed using FlowJo software (v. 10). Expression of each marker in HMDM, which was gated according to FSC/SSC properties, was shown in histogram ((a) siControl, blue line; siATP8B1, red line; isotype control, black line, (b) control subjects, blue line; PFIC1 patients, red line; isotype control, black line). A representative result of two independent experiments (a) and two PFIC1 patients (no.3 and no.4) (b) is shown.

Supporting Fig. 3. Reduced mRNA expression of M2c markers, CD163 and CD14, by ATP8B1 suppression.

HMDM transfected with siControl or siATP8B1 were generated as described in Fig. 2. The cells were subjected to RNA preparation and then analyzed by qPCR. The expression of *CD163, CD14, and CD16* in each reaction was normalized to that of *ACBT*. Data are shown as means ± SEM of quadruplicate determinations. *, $P<0.05$, **, $P<0.01$, ***, $P<0.001$ versus nonpolarized HMDM; $^{\#}$, $P<0.05$, $^{\#\#\#}$, $P<0.001$ versus siControl. A representative result of four independent experiments is shown.

Supporting Fig. 4. M2c have lower SSC than the other subtypes comprising IL-10-driven HMDM.

HPBMo were seeded, differentiated into HMDM by culture for 4 days in RPMI/M-CSF, and then cultured in RPMI/M-CSF with IL-10 (40 ng/ml) for 6 days to elicit M2c polarization. The IL-10-driven HMDM were subjected to flow cytometric analysis, gated according to FSC/SSC properties as described in Supporting Fig. 2, and divided into $CD163^{+}CD14^{+}CD16^{+}$ cells (M2c) and the other cells using FlowJo software (v. 10). Both subsets are shown as histograms with SSC (a) and the mean SSC was calculated and is presented as relative to that in IL-10-driven HMDM (b). Data shown are means ± SEM of triplicate determinations. **, $P<0.01$. A representative result of four independent experiments is shown.

Supporting Fig. 5. Composition of HPBMo subsets in PFIC patients and control subjects.

HPBMo from control subjects or PFIC patients were stained with fluorochrome-labeled antibodies against CD14 and CD16, subjected to flow cytometry, and analyzed using FlowJo software (v. 10). HPBMo was gated according to FSC/SSC properties and divided into three subsets, $CD14^{++}CD16^{-}$, $CD14^{++}CD16^{+}$, and $CD14^{dim}CD16^{+}$, on the basis of expression levels of CD14 and CD16. Quadrants and numbers in contour plot

indicate percentage of cells in each gate.

Supporting Table 1. Antibody list

Antigen	Label	Source	Company	Catalog No.	RRID	Application
CD163	unconjugated	rabbit polyclonal	Santa Cruz Biotechnology	sc33559	AB_2074552	IB
CD23	unconjugated	rabbit monoclonal	Abcam	ab92495	AB_10562095	IB
CD80	unconjugated	mouse monoclonal	BD Pharmingen	557223	AB_396602	ICC
CD93	unconjugated	goat polyclonal	R&D systems	AF2379	AB_416584	ICC
MerTK	unconjugated	goat polyclonal	R&D systems	AF891	AB_355691	IB
25F9	unconjugated	mouse monoclonal	eBioscience	14-0115-82	AB_953652	ICC
IL-10Rα	unconjugated	rabbit polyclonal	Santa Cruz Biotechnology	sc984	AB_631786	IB
STAT3	unconjugated	mouse monoclonal	Cell Signaling technology	9139	AB_331757	IB
STAT3α	unconjugated	rabbit monoclonal	Cell Signaling technology	8768	NA	IB
phospho-Stat3 (Tyr705)	unconjugated	rabbit monoclonal	Cell Signaling technology	9145	NA	IB
phospho-Stat3 (Ser727)	unconjugated	rabbit polyclonal	Cell Signaling technology	9134	NA	IB
FLAG	unconjugated	rabbit polyclonal	Sigma-Aldrich	F3165	AB_259529	IB, ICC
HA	unconjugated	rat monoclonal	Roche	11867431001	AB_390919	IB
α1 Na^+, K^+-ATPase	unconjugated	mouse monoclonal	Abcam	ab7671	AB_306023	IB, ICC
β-actin	unconjugated	mouse monoclonal	MP biomedicals	69100	AB_2335127	IB
EEA1	unconjugated	rabbit polyclonal	Abcam	ab2900	AB_2262056	IB
Histon H3	unconjugated	mouse monoclonal	MAB Institute	MA301A	NA	IB
CD14	APC	mouse monoclonal	BioLegend	325602	AB_830675	FC
CD16	PE	mouse monoclonal	BioLegend	302008	AB_314208	FC
CD163	FITC	mouse monoclonal	BioLegend	333618	AB_2563094	FC
CD163	APC	mouse monoclonal	BioLegend	333610	AB_2074533	FC
CD68	FITC	mouse monoclonal	BD Pharmingen	562117	AB_10896283	FC
CD83	APC	mouse monoclonal	BD Pharmingen	551073	AB_398488	FC
CD93	PE	mouse monoclonal	MBL	D198-5	AB_10209280	FC
MerTK	PE	mouse monoclonal	R&D systems	FAB8912P	AB_357214	FC

IB, immunoblotting; ICC, immunocytochemistry; FC, flow cytometric analysis; NA, not applicable

Supporting Table 2. Primers for Q-PCR

Gene	Forwared (5' to 3')	Reverse (5' to 3')
ATP8B1	ATGCAAGGATGGAAAACCAG	CGCATCCGTCTTTCTTCTTC
CD163	TTGCCAGCAGCTTAAATGTG	AGGACAGTGTTTGGGACTGG
CD14	CTGCAACTTCTCCGAACCTC	CCAGTAGCTGAGCAGGAACC
CD16	CCTCCCAACTGCTCTGCTAC	AGCACCCTGTACCATTGAGG
SOCS3	GCTCCAAGAGCGAGTACCAG	GACTGGGTCTTGACGCTGAG
ZFP36	CTTCAGCGCTCCCACTCTCGG	CGTCAGGGCTCAGCGACAGGA
SBNO2	AAAGACCTGCGACTTTGCTC	GGACGAGGAGAAGATGGAGA
ACTB	GGACTTCGAGCAAGAGATGG	AGGAAGGAAGGCTGGAAGAG

Supporting Figure 1

a.

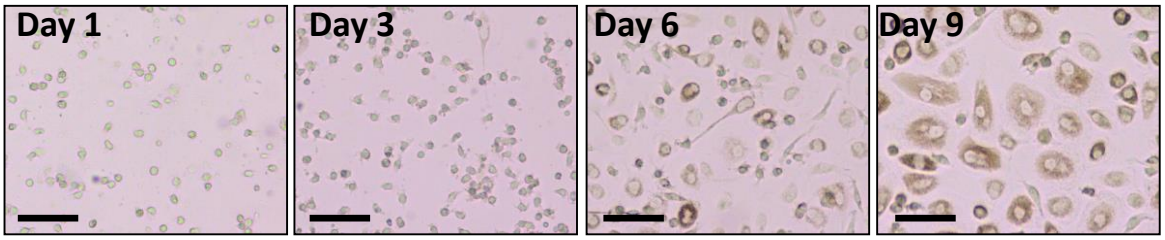

b.

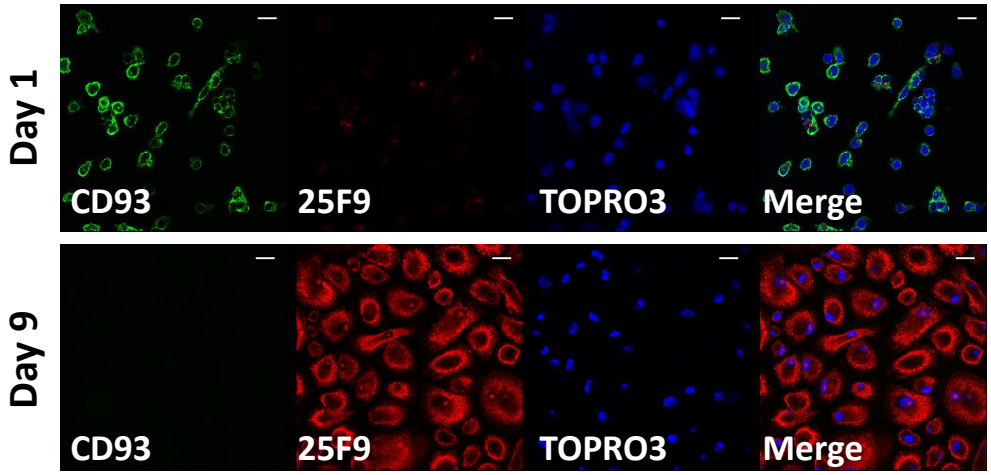

c.

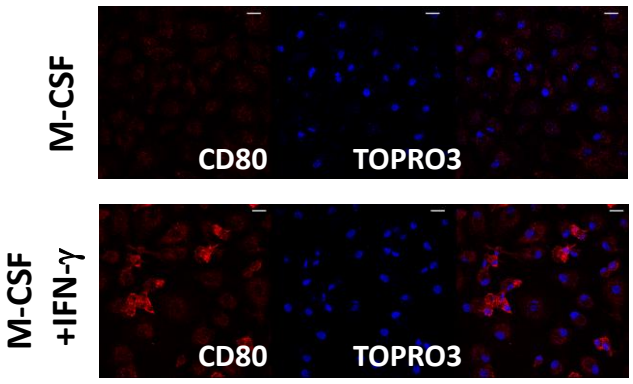

Supporting Figure 2

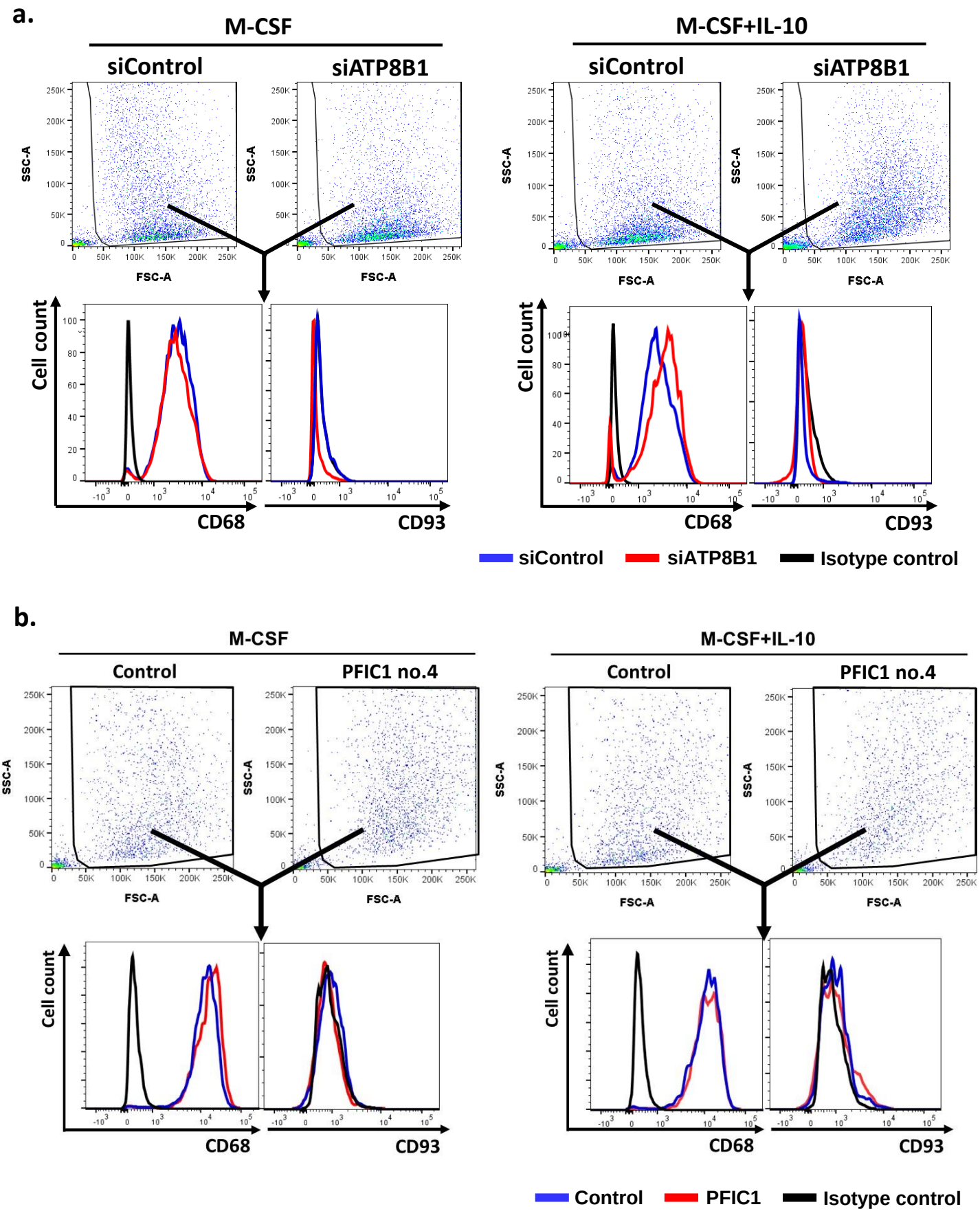

Supporting Figure 3

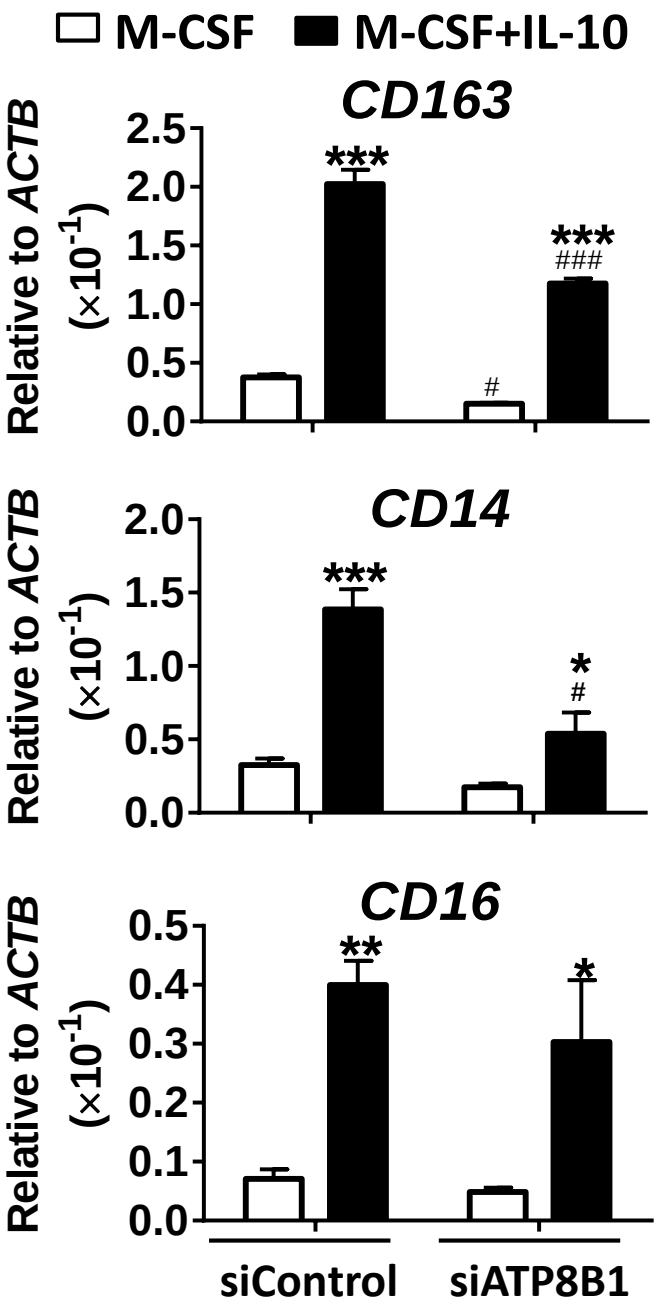

Supporting Figure 4

a.

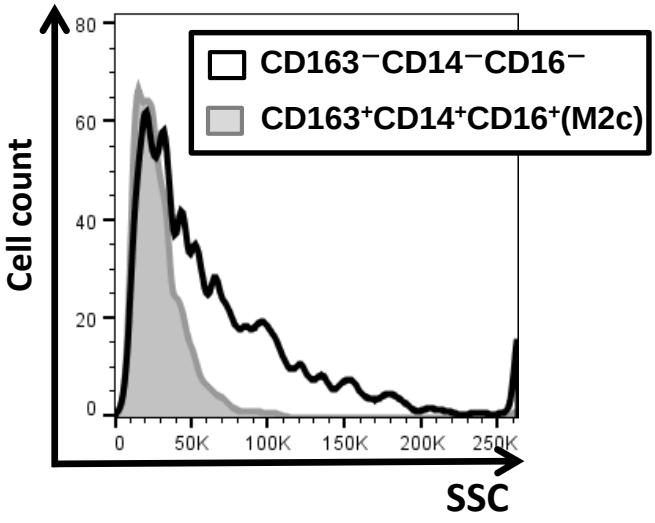

b.

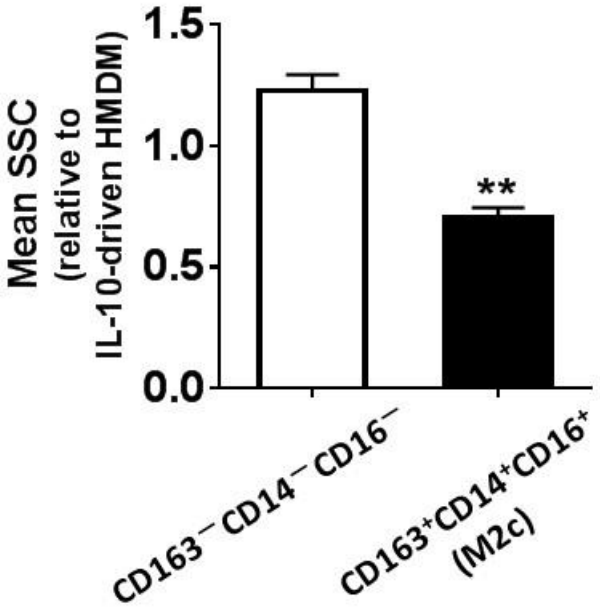

Supporting Figure 5